This is the author's peer reviewed,

10

11

12

13

14

15

16

17

18

19

21

22

23

24

26

27

29

30

31

32

33

34

35

36

37

38

39

40 41

42

43

44 45

47

48

49

51 52

accepted manuscript. However, the online version of record will be different from this version once it has been copyedited and typeset

PLEASE CITE THIS ARTICLE AS DOI: 10.1063/5.0097177

Non-Hermitian Planar Elastic Metasurface for Unidirectional Focusing of Flexural Waves

Katerina Stojanoska¹, Chen Shen^{1,a1}

Department of Mechanical Engineering, Rowan University, Glassboro, NJ 08028, USA

a) Author to whom correspondence should be addressed: shenc@rowan.edu

(Dated: 23 May 2022)

Metasurfaces exhibiting spatially asymmetric inner structures have been shown to host unidirectional scattering effects, benefiting areas where directional control of waves is desired. In this work, we propose a non-Hermitian planar elastic metasurface to achieve unidirectional focusing of flexural waves. The unit cells are constructed by piezoelectric disks and metallic blocks that are asymmetrically loaded. A tunable material loss is then introduced by negative capacitance shunting. By suitably engineering the induced loss profile, a series of unit cells are designed, which can individually access the exceptional points (EPs) manifested by unidirectional zero reflection. We then construct a planar metasurface by tuning the reflected phase to ensure constructive interference at one side of the metasurface. Unidirectional focusing of the incident waves is demonstrated, where the reflected wave energy is focused from one direction and zero reflection is observed in the other direction. The proposed metasurface enriches the flexibility in asymmetric elastic wave manipulation as the loss and the reflected phase can be tailored independently in each unit cell.

The notion of parity-time (PT) symmetry was first proposed 56 by Bender and Boettcher in 1998¹, where it is found that the 57 behavior of PT-symmetric systems can change dramatically at 58 a state transition from real to complex energies. At this point, 59 the symmetry of the system would be broken, and real spec- 60 tra in the Hamiltonian are achieved. A necessary condition 61 for PT-symmetry is that for the Hamiltonian potential, it must 62 be even in its real part and odd in its imaginary part. Once 63 the imaginary part reaches a certain threshold, a break in PT 64 symmetry can be observed which causes an abrupt change in 65 the real energy spectrum²⁻⁴. This transition corresponds to an ₆₆ exceptional point (EP) where the eigenstates become degen-67 erate. Thanks to the mathematical equivalence between the 68 Schrodinger's equation and the paraxial electromagnetic wave 69 equations^{2,5}, the study of EP has been extended to a plethora 70 of physical systems other than quantum mechanics. Such 71 systems comprise acoustics^{6–11}, optics^{12–19}, photonics^{20–25}, among many others.

Recently, in the field of acoustics and elastodynamics, it 74 is found that the occurrence of EP could be related to Willis 75 coupling²⁶⁻²⁸ where a cross-coupling between stress and ve-76 locity or momentum and strain exists. To achieve this phe-77 nomenon, the eigenstates of the scattering matrix must coa-78 lesce. Due to the fascinating effects the Willis coupling pos-79 sesses, there has been an upsurge of interest in this area in 80 recent years^{29–32}. For example, perfect wavefront transfor-81 mation with 100% conversion efficiency has been proposed 82 based on the concept where the input energy is directed to the 83 intended direction without diffraction or scattering into un- 84 desirable directions^{33–35}. In the field of elastic waves, such 85 a coupling effect has also been found in non-destructive test- ${\tt s6}$ ing and structural-health monitoring ${\tt ^{36,37}}.$ Willis coupling typ- ${\tt ^{87}}$ ically takes place when the structures are geometrically asym-88 metric. It is found that when loss is added to the system 89 and a non-Hermitian description is needed, EPs can be engi-90 neered by carefully tailoring the loss and the structure asym-91 metry such that unidirectional zero reflection is achieved²⁶.92 Recent studies have shown that Willis material can be used 93 for manipulating flexural waves using artificial structures²⁸ as 94

well as for constructing unidirectional reflectionless acoustic devices²⁷ to achieve purposeful sound insulation and steering. However, existing metasurfaces that host EPs either do not have planar geometry or are difficult to individually control the loss profile in their unit cells, limiting their practical usage in different scenarios.

In this paper, we are extending the concept by proposing a planar non-Hermitian elastic metasurface for the control of flexural waves. With the loss being induced by negative capacitance piezoelectric shunting, symmetry breaking takes place followed by an emergence of EPs. The numerical simulations show strong asymmetric reflection properties, i.e., zero reflection in the immediate vicinity of the EPs when the structure is ensonified from one side. Additionally, with the waves being incident on the other side, there is an occurrence of focusing of the waves. Thus, a desired asymmetric control of flexural waves can be achieved with the planar elastic metasurface. The loss can be conveniently tuned by varying the negative capacitance shunting of the piezoelectric disks, thus enabling other potential applications.

We consider flexural wave propagation on a thin elastic beam made of acrylic. The geometry of the building block is shown in Fig.1a, where a cavity is perforated on the beam and a piezoelectric disk and a metallic block are connected in series. In this way, the unit cell is loaded asymmetrically since the piezoelectric disk is only attached to one side of the cavity. As shown in previous works^{26,28}, this spatial asymmetry can lead to different scattering properties for waves incident from opposite directions. To achieve a larger degree of asymmetry, each unit cell of the metasurface is composed of five individual building blocks, as illustrated in Fig.1b. We define the forward direction when the piezoelectric disk is placed in front of the metallic block. Here the piezoelectric material is chosen as Lead Zirconate Titanate (PZT-5H) with dimensions being $l_p = 1$ mm, $w_p = 3$ mm, and $h_p = 0.585$ mm. The metallic block is made of lead with $l_1 = 1.5$ mm, $w_1 = 3$ mm, and h_1 = 3.9 mm and the size of the acrylic beam building block is l_a = 5 mm, w_a = 6 mm, and h_a = 2 mm. The total length of the unit cell of the metasurface is therefore 25 mm.

accepted manuscript. However, the online version of record will be different from this version once it has been copyedited and typeset This is the author's peer reviewed,

PLEASE CITE THIS ARTICLE AS DOI: 10.1063/5.0097177

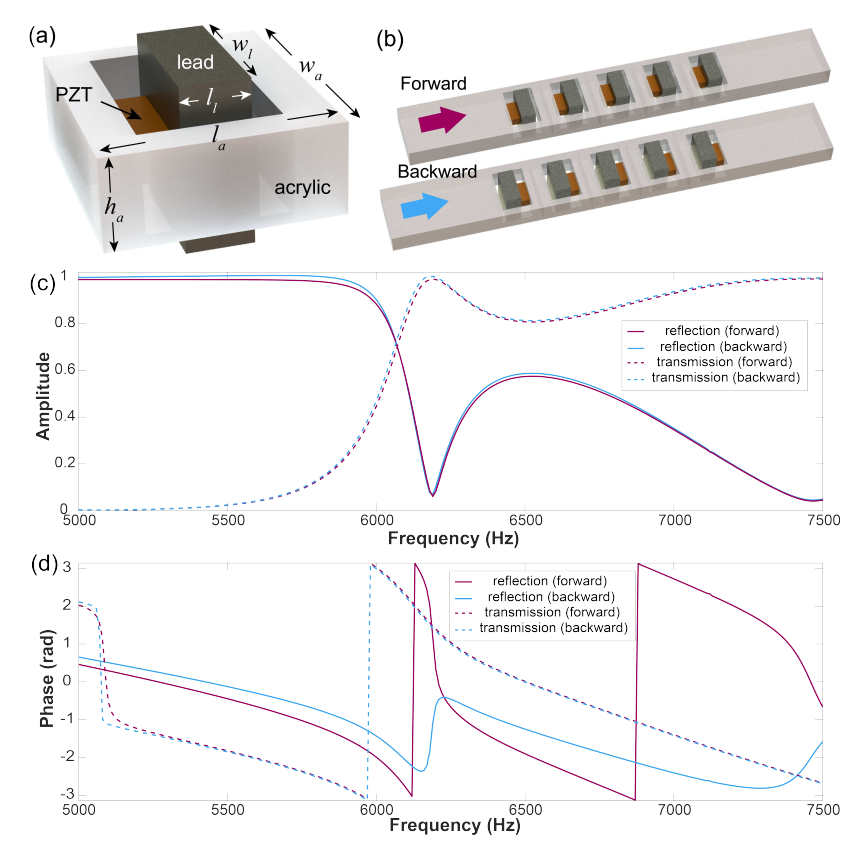


FIG. 1. (a) Schematic view of one resonating building block. (b) Forward and backward view of the unit cell with given directions of the flexural waves. (c) Amplitude of the reflection and transmission coefficients for the flexural wave propagating in forward and backward directions. (d) Phase shift of the reflection and transmission coefficients for the flexural wave propagating in forward and backward directions.

The amplitude and the phase of the reflection and trans-123 mission coefficients are shown in Figs.1c and 1d. It is ex_{124} pected that the amplitude of the reflected and transmitted wave2s should be the same regardless of the propagation direction of20

the waves as the structure is entirely passive and lossless. The slight difference is likely caused by the numerical errors in the simulations. The reflected phase, on the other hand, is different depending on the incident wave direction, which is a result of the structural asymmetry of the unit cells.

To further break the symmetry of the system, loss is added to the structures. The introduction of loss will make the system non-Hermitian as manifested by the change of the reflection amplitudes. Here the loss is induced by a shunted circuit connected to the piezoelectric disk 36,38 . The effective Young's modulus, including the loss factor, can be modified by applying the negative capacitance shunting circuit, which is shown in Fig.2a. The equivalent capacitance C_n realized by the circuit can be tuned by the R_1 , R_2 and C values, and the modified effective Young's modulus is expressed as 38 :

accepted manuscript. However, the online version of record will be different from this version once it has been copyedited and typeset

This is the author's peer reviewed,



127

128

129

130

131

132

133

134

135

136

137

138

139

141

142

143

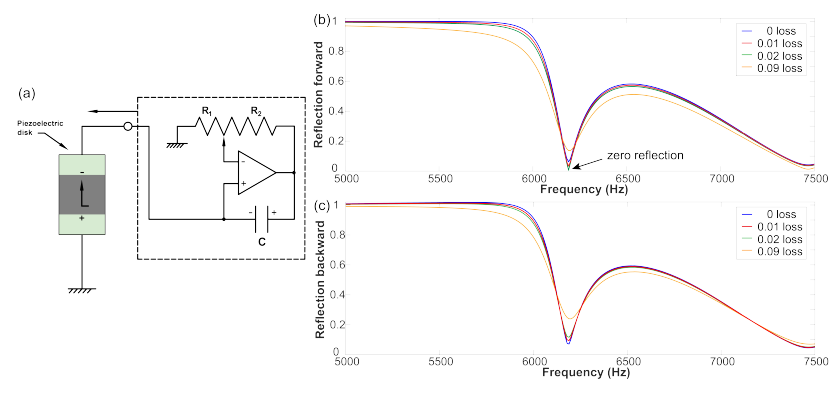


FIG. 2. (a) Piezoelectric disk connected to a negative capacitance shunting circuit. (b) Amplitude of the reflection coefficient for the flexural wave propagating in a forward direction for different loss patterns. (c) Amplitude of the reflection coefficient for the flexural wave propagating in a backward direction for different loss patterns

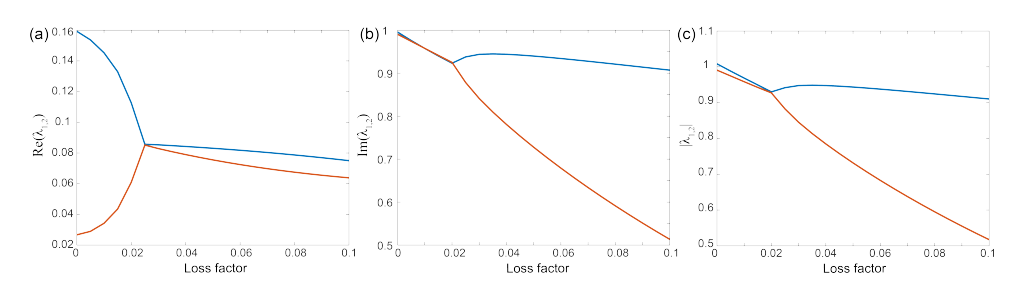


FIG. 3. Real (a), imaginary (b), and absolute value (c) of the eigenvalues of the S matrix at 6190 Hz.

145

$$E_P = E_P^{\rm E} \frac{C_P^{\rm T} - C_n}{C_P^{\rm T} (1 - k_{31}^2) - C_n} \tag{1)47}$$

where $C_p^{\rm T}$, C_n , $E_p^{\rm E}$, and k_{31} represent the capacitance of the piezoelectric disk, the capacitance of the circuit, the short circles cuit modulus, and the electromechanical coupling coefficient respectively.

The loss can thus be conveniently tuned by the shunting resistance and the negative capacitance. Compared to other approaches such as attaching a soft porous rubber to the beam²⁷ it provides an easy means to tune the loss of the PZT. This will greatly facilitate the design of the unit cells as well as the metasurface since the loss profile needs to be carefully adjusted, as will be shown later. It is important to point out that 160 the intrinsic loss of the host beam is not considered in the simulation. If necessary, the induced loss by negative capacitance shunting can be adjusted such that the overall loss leads to zero reflection from the forward direction.

As shown in Fig.2b, at the resonance frequency of 6190 Hz₁₆₅ the reflection amplitude of the wave propagating in the forward direction is finite when the system is lossless. The am-

plitude changes as we increase the loss factor monotonically. Remarkably, when a loss factor of 0.02 is introduced, the unit cell exhibits unidirectional zero reflection, i.e., the reflection amplitude approaches zero in the forward direction while it is finite in the backward direction. Furthermore, when the loss factor passes this critical value, the amplitude is changed and is no longer zero. In addition, when we are taking into consideration the propagating wave being incident from a backward direction as illustrated in Fig.2c, it is obvious that the amplitude is the same as the amplitude of the wave propagating in a forward direction when the system is assumed lossless. To additionally elaborate, an introduction of a particular loss at the same frequency of 6190 Hz clearly shows that the reflection amplitudes for the propagating wave in the backward direction differ from the forward representing an asymmetry, thus the reflection never reaches zero. At this point, it is obvious as expected that the scattering matrix no longer remains unitary. It is important to point out that the transmission amplitudes of the propagating wave stay the same regardless of the amount of the added loss because the system is reciprocal albeit it is lossy. To further confirm the behavior at this frequency and its relation to EP, the eigenvalues of the scattering matrix are



Applied Physics Letters

accepted manuscript. However, the online version of record will be different from this version once it has been copyedited and typeset PLEASE CITE THIS ARTICLE AS DOI: 10.1063/5.0097177 This is the author's peer reviewed,

167

168

169

170

171

172

173

174

175

176

177

178

179

180

181

183

184

185

186

187

188

189

191

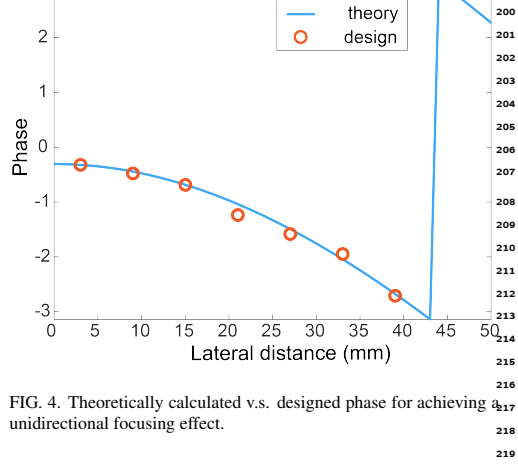
192

193

195

196

197



3

calculated as a function of the induced loss factor at 6190 Hz₂₂₁ and the results are presented in Fig.3. It can be seen that when the loss factor is funed to 0.02, there is a coalescence of the $_{223}$ real and the imaginary part of the eigenvalues. A biased dis-224 tribution is observed before and after the occurrence of the EP₂₂₅ in Figs.3a and 3b, respectively for the real and the imaginary₂₂₆ part. The absolute values also undergo a phase transition at 227 this point. As such, the two eigenstates become degenerate as shown in Fig.3c. This peculiar behavior is a clear sign of the emergence of EP in the system.

A metasurface is further designed to achieve a unidirec-231 tional focusing effect. This is achieved by designing a series 232 of unit cells that all host EP in the forward direction but have different reflected phases in the backward direction. From 234 previous simulations, we have confirmed that the wavelength of the flexural wave is $\lambda = 30.66$ mm at 6190 Hz, the width of the unit cells, on the other hand, is $w_a = 6$ mm which is about₂₃₇ 1/5 of the wavelength. This helps to achieve enough spatial 238 resolution of the metasurface. The focal distance is assumed $_{239}$ to be d = 60 mm, and the required phase of the metasurface is₂₄₀ calculated by the constructive interference at the focal point: 241

$$\phi=2\pi\frac{\sqrt{d^2+\Delta x^2}-d}{\lambda} \hspace{1cm} (2)_{244}^{243}$$

where Δx is the lateral distance from the center of the meta-246 surface. The required phase is illustrated by the blue curve47 in Fig.4, while the red circles mark the actual phase of the48 designed unit cells. A total number of eight unit cells are de-249 signed which cover a phase shift of around π . The geometry₂₅₀ of each unit cell is obtained by tuning the height of the metal-251 lic blocks as well as the piezoelectric disks while keeping these unidirectional zero reflection behavior. The corresponding di-253 mensions and the associated loss factors for each unit cell ares given in Table I. It should be noted that the loss factors areas different for each individual unit cell in order to achieve EP256 In other words, the loss profile of the entire metasurface needs to be carefully modulated such that all the unit cells can access their respective EP. The negative capacitance shunting mechanism provides a convenient means to adjust the loss in each unit without physically altering the structure or adding additional materials. The designed metasurface consists of sixteen resonator-based unit cells, placed symmetrically about the center of the metasurface, in order to achieve a unidirectional focusing effect.

200

202 203

205

207

209

210

211

212

215

242

Fig.5a shows that when the flexural wave is excited in the forward direction at 6190 Hz, the wavefront remains planar, and very little interference is observed on the reflection side, which indicates zero reflection is achieved. This is because each unit cell is tailored to exhibit EP at the operation frequency, hence net-zero reflection is achieved for the entire metasurface. On the other hand, the interference pattern is vastly different for flexural waves propagating from the opposite direction. Different local reflection coefficients are induced at the unit cells, and focusing of reflected waves is achieved based on constructive interference at the far-field. Such phenomenon is confirmed by Fig.5b, which displays a focusing pattern. The focal point is around 55 mm away from the metasurface, which is slightly different from the designed value as d = 60mm. This can be explained by the non-ideal reflected phase and the coupling and interactions among the unit cells. Nevertheless, the metasurface exhibits strong asymmetric scattering properties that could be of great importance where directional wave manipulation is desired. As for the difference on the transmission side, it is likely caused by the diffractions at the metasurface since its width is much larger than the corresponding wavelength. This is similar to the case where a wide waveguide that supports multiple modes can lead to different transmission patterns for incident wave from different directions³⁹. It should be noted that, however, such an asymmetry does not break the reciprocity of the system. Moreover, to quantitatively evaluate the focusing effect by the metasurface, the displacement amplitude of the reflected waves is extracted at a distance of d = 55 mm away from the metasurface. The result is shown in Fig.5c and a clear focal profile is observed. The full width at half maximum (FWHM) is around 0.83λ . The focusing effect may be further increased by improving the design, e.g., with more unit cells that cover a larger phase shift.

To conclude, we have proposed a non-Hermitian planar elastic metasurface for a unidirectional focusing effect using Willis materials. The metasurface contains piezoelectric materials and metallic blocks that are asymmetrically loaded and the loss is introduced by the shunted piezos. The proposed design works for flexural waves on elastic structures. Unidirectional zero reflection is achieved when approaching the EP of the scattering matrix in the unit cells by tuning the losses, which are represented as a non-Hermitian system. Furthermore, a unidirectional focusing effect is achieved based on a metasurface composed of a series of unit cells. The backward propagation of the waves shows that there is a focus of the wave energy due to the constructed phase of the reflection waves while negligible reflection is observed from the other side. Compared to curved metasurfaces that achieve similar

accepted manuscript. However, the online version of record will be different from this version once it has been copyedited and typeset This is the author's peer reviewed,

PLEASE CITE THIS ARTICLE AS DOI: 10.1063/5.0097177

257

258

259

260

261

262

263

264

265

266 267

268

269

270

271

272

273

274

275

Unit cell number	Height of lead [mm]	Height of PZT [mm]	Loss factor
1	6.5	1.56	0.05
2	6.0	1.21	0.04
3	5.5	1.01	0.04
4	3.9	0.59	0.02
5	3.5	0.51	0.02
6	2.8	0.41	0.02
7	2.2	0.34	0.02
8	2.0	0.32	0.01

TABLE I. Corresponding dimensions and loss factors for each unit cell.

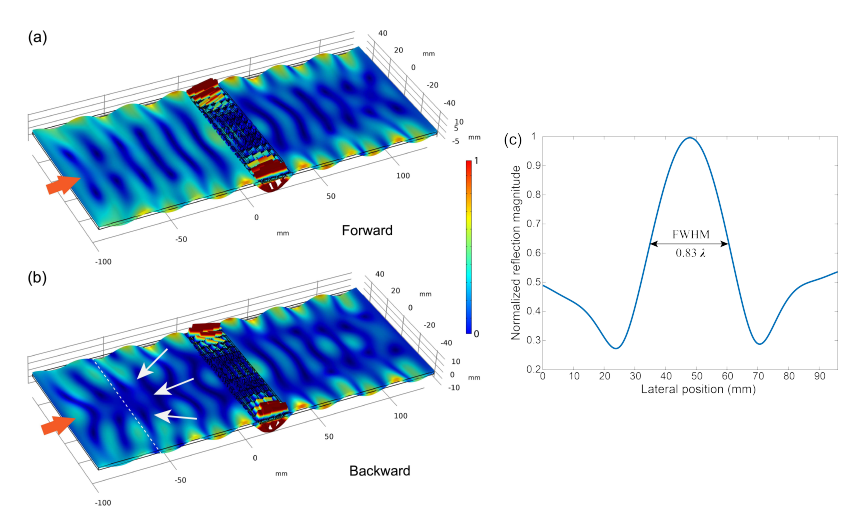


FIG. 5. (a) Displacement magnitude of the metasurface with incident waves in the forward direction. (b) Displacement magnitude of the metasurface with incident waves in the backward direction. (c) Normalized reflection magnitude from the cutline at d = 55mm.

effects⁴⁰, the compact and planar structure is easy to be inte-277 grated into existing structures and can be applied in various278 scenarios. The ability to tune the unit cells individually offers a greater design degree of freedom by controlling the reflections from different directions. For example, other unidirec-279 tional wave devices can be synthesized by engineering the reflected phase based on the same concept to achieve other types of beam engineering, e.g., beam steering, accelerating beams, and so on. The proposed mechanism can be also used in different types of elastic waves, such as bulk and surface waves281 by the means of a suitable design and introduction of loss. As of experimental implementation, a potential challenge is the complexity of the metasurface due to the individual tuning,82 of the unit cells and external circuits⁴¹. It is hoped that the proposed system will bring about additional possibilities for $_{283}$ elastic wave manipulation for applications in structural health monitoring and non-destructive testing. Further improvement of the design may be done by optimization of the unit cells to be able to cover a full phase shift of 2π to achieve other₂₈₆ functionalities.

This material is based on work supported by the National Science Foundation under Grant No. 2137749.

AUTHOR DECLARATIONS

Conflict of Interest

The authors have no conflicts to disclose.

DATA AVAILABILITY

The data that support the findings of this study are available from the corresponding author upon reasonable request.

¹C. M. Bender and S. Boettcher, "Real spectra in non-hermitian hamiltonians having p t symmetry," Physical review letters **80**, 5243 (1998).

²C. M. Bender, "Making sense of non-hermitian hamiltonians," Reports on Progress in Physics **70**, 947 (2007).



ACCEPTED MANUSCRIPT

Applied Physics Letters



This

accepted manuscript. However, the online version of record will be different from this version once it has been copyedited and typeset author's peer reviewed, is the

PLEASE CITE THIS ARTICLE AS DOI: 10.1063/5.0097177

Feng, R. El-Ganainy, and L. Ge, "Non-hermitian photonics based onb46 parity-time symmetry," Nature Photonics 11, 752–762 (2017).
 El-Ganainy, K. G. Makris, M. Khajavikhan, Z. H. Musslimani, S. Rots48

289

290

292

293 294

295

296

297

298

299

300

301

302

303

304

305

306

307

308

309

310

311

312

313

314

315

316

317

318

319

320

321

322 323

324

325

327

328

329

331

332

334

335

337

338

340

341

343

344

⁴R. El-Ganainy, K. G. Makris, M. Khajavikhan, Z. H. Musslimani, S. Rotsaster, and D. N. Christodoulides, "Non-hermitian physics and pt symmetry," 349 Nature Physics 14, 11–19 (2018).

⁵C. M. Bender, D. C. Brody, and H. F. Jones, "Complex extension of quan-ss1 tum mechanics," Physical Review Letters 89, 270401 (2002).

⁶X. Zhu, H. Ramezani, C. Shi, J. Zhu, and X. Zhang, "Pt-symmetric acous₃₅₃ tics," Physical Review X **4**, 031042 (2014).

⁷R. Fleury, D. Sounas, and A. Alu, "An invisible acoustic sensor based onbss parity-time symmetry," Nature communications **6**, 1–7 (2015).

⁸C. Shi, M. Dubois, Y. Chen, L. Cheng, H. Ramezani, Y. Wang, andsr X. Zhang, "Accessing the exceptional points of parity-time symmetric, acoustics," Nature communications 7, 1–5 (2016).

⁹J. Christensen, M. Willatzen, V. Velasco, and M.-H. Lu, "Parity-time syn₃₆₀ thetic phononic media," Physical review letters 116, 207601 (2016).

¹⁰V. Achilleos, G. Theocharis, O. Richoux, and V. Pagneux, "Non-hermitialbe2 acoustic metamaterials: Role of exceptional points in sound absorption," 363 Physical Review B 95, 144303 (2017).

¹¹Y. Zhou, Z.-Z. Yang, Y.-Y. Peng, and X.-Y. Zou, "Pt-symmetric acoustic₃₆₅ system constructed by piezoelectric composite plates with active external₃₆₆ circuits," Chinese Physics B (2022).
³⁶⁷

12A. Guo, G. Salamo, D. Duchesne, R. Morandotti, M. Volatier-Ravatases
 V. Aimez, G. Siviloglou, and D. Christodoulides, "Observation of pt 369 symmetry breaking in complex optical potentials," Physical review letters, 103, 093902 (2009).

¹³C. E. Rüter, K. G. Makris, R. El-Ganainy, D. N. Christodoulides, M. Segev₃₇₂ and D. Kip, "Observation of parity–time symmetry in optics," Nature₃₇₃ physics 6, 192–195 (2010).

physics 6, 192–195 (2010).

14Z. Lin, H. Ramezani, T. Eichelkraut, T. Kottos, H. Cao, and D. N₃₇₅

Christodoulides, "Unidirectional invisibility induced by p t-symmetric pe 376

riodic structures," Physical Review Letters 106, 213901 (2011).

377

¹⁵L. Feng, Y.-L. Xu, W. S. Fegadolli, M.-H. Lu, J. E. Oliveira, V. R. Almeida₉₇₈ Y.-F. Chen, and A. Scherer, "Experimental demonstration of a unidirec₃₇₉ tional reflectionless parity-time metamaterial at optical frequencies," Na₃₈₀ ture materials 12, 108–113 (2013).

¹⁶J. Wen, X. Jiang, L. Jiang, and M. Xiao, "Parity-time symmetry in optical sagmicrocavity systems," Journal of Physics B: Atomic, Molecular and Optical sagmicrocavity systems, "Journal of Physics B: Atomic, Molecular and Optical sagmics," June 2011, 202001 (2018).

¹⁷M. Moccia, G. Castaldi, F. Monticone, and V. Galdi, "Exceptional points in sefflat optics: A non-hermitian line-wave scenario," Physical Review Applied 86 15, 064067 (2021).

¹⁸J. Xie, S. Dong, B. Yan, Y. Peng, C. Qiu, S. Wen, et al., "Simple the 388 oretical model for parity-time-symmetric metasurfaces," arXiv preprint, arXiv:2107.10506 (2021).
³⁹⁰
¹⁹L. Wang, F. Liu, F. Liu, Z. Qin, Y. Zhang, D. Zhong, and H. Ni, "Optical statement of the control of the

¹⁹L. Wang, F. Liu, F. Liu, Z. Qin, Y. Zhang, D. Zhong, and H. Ni, "Optical₉₁ fractal and exceptional points in pt symmetry thue-morse photonic multi₃₉₂ layers," Optical Materials 123, 111821 (2022).

²⁰ A. Regensburger, C. Bersch, M.-A. Miri, G. Onishchukov, D. N₃₉₄ Christodoulides, and U. Peschel, "Parity-time synthetic photonic lattices," 3₉₅ Nature 488, 167–171 (2012).

Nature 488, 167–171 (2012).

21Y. Lumer, Y. Plotnik, M. C. Rechtsman, and M. Segev, "Nonlinearly induced p t transition in photonic systems," Physical review letters 111 398 263901 (2013).

²² B. Peng, Ş. K. Özdemir, F. Lei, F. Monifi, M. Gianfreda, G. L. Long, S. Fanano, F. Nori, C. M. Bender, and L. Yang, "Parity-time-symmetric whispering 401 gallery microcavities," Nature Physics 10, 394–398 (2014).

²³M. Lawrence, N. Xu, X. Zhang, L. Cong, J. Han, W. Zhang, and S. Zhang, "Manifestation of p t symmetry breaking in polarization space with terahertz metasurfaces," Physical review letters 113, 093901 (2014).

6

²⁴M. Wu, F. Liu, D. Zhao, and Y. Wang, "Unidirectional invisibility in pt-symmetric cantor photonic crystals," Crystals 12, 199 (2022).

²²N. Maraviglia, P. Yard, R. Wakefield, J. Carolan, C. Sparrow, L. Chakhmakhchyan, C. Harrold, T. Hashimoto, N. Matsuda, A. K. Harter, et al., "Photonic quantum simulations of coupled pt-symmetric hamiltonians," Physical Review Research 4, 013051 (2022).

²⁶C. Shen, J. Li, X. Peng, and S. A. Cummer, "Synthetic exceptional points and unidirectional zero reflection in non-hermitian acoustic systems," Physical Review Materials 2, 125203 (2018).

²⁷A. Merkel, V. Romero-García, J.-P. Groby, J. Li, and J. Christensen, "Unidirectional zero sonic reflection in passive pt-symmetric willis media," Physical Review B 98, 201102 (2018).

²⁸Y. Liu, Z. Liang, J. Zhu, L. Xia, O. Mondain-Monval, T. Brunet, A. Alù, and J. Li, "Willis metamaterial on a structured beam," Physical Review X 9, 011040 (2019).

²⁹S. Koo, C. Cho, J.-h. Jeong, and N. Park, "Acoustic omni meta-atom for decoupled access to all octants of a wave parameter space," Nature communications 7, 1–7 (2016).

mications 7, 1–7 (2016).
3ºM. B. Muhlestein, C. F. Sieck, P. S. Wilson, and M. R. Haberman, "Experimental evidence of willis coupling in a one-dimensional effective material

element," Nature communications **8**, 1–9 (2017).

³¹C. F. Sieck, A. Alù, and M. R. Haberman, "Origins of willis coupling and acoustic bianisotropy in acoustic metamaterials through source-driven

homogenization," Physical Review B **96**, 104303 (2017).

32X. Su and A. N. Norris, "Retrieval method for the bianisotropic polarizability tensor of willis acoustic scatterers," Physical Review B **98**, 174305

(2018).
³³A. Díaz-Rubio and S. A. Tretyakov, "Acoustic metasurfaces for scattering-free anomalous reflection and refraction." Physical Review B 96, 125409

³⁴J. Li, C. Shen, A. Díaz-Rubio, S. A. Tretyakov, and S. A. Cummer, "Systematic design and experimental demonstration of bianisotropic metasurfaces for scattering-free manipulation of acoustic wavefronts," Nature communications 9, 1–9 (2018).

35L. Quan, Y. Ra'di, D. L. Sounas, and A. Alù, "Maximum willis coupling in acoustic scatterers," Physical Review Letters 120, 254301 (2018).

³⁶Z. Chen, M. Negahban, Z. Li, and J. Zhu, "Tunable exceptional point and unidirectional zero reflection of a metabeam using shunted piezos," Journal of Physics D: Applied Physics 53, 095503 (2019).

³⁷X. Li, Z. Yu, H. Iizuka, and T. Lee, "Experimental demonstration of extremely asymmetric flexural wave absorption at the exceptional point," Extreme Mechanics Letters 52, 101649 (2022).

³⁸Y. Chen, G. Huang, and C. Sun, "Band gap control in an active elastic metamaterial with negative capacitance piezoelectric shunting," Journal of Vibration and Acoustics 136 (2014).

³⁹J. Zhu, X. Zhu, X. Yin, Y. Wang, and X. Zhang, "Unidirectional extraordinary sound transmission with mode-selective resonant materials," Physical Review Applied 13, 041001 (2020).

⁴⁰T. Liu, X. Zhu, F. Chen, S. Liang, and J. Zhu, "Unidirectional wave vector manipulation in two-dimensional space with an all passive acoustic paritytime-symmetric metamaterials crystal," Physical review letters 120, 124502 (2018).

⁴ X. Li, Y. Chen, R. Zhu, and G. Huang, "An active meta-layer for optimal flexural wave absorption and cloaking," Mechanical Systems and Signal Processing 149, 107324 (2021).



This is the author's peer reviewed, accepted manuscript. However, the online version of record will be different from this version once it has been copyedited and typeset. (a) (b) W_a lead Forward PZT **Backward** acrylic PLEASE CITE THIS ARTICLE AS DOI: 10.1063/5.0097177 $(c)^{1}$ 8.0 reflection (forward) reflection (backward) Amplitude 0.4 transmission (forward) transmission (backward) 0.2 Frequency (Hz) 0 5000 6500 7000 5500 (d)₃ reflection (forward) reflection (backward) 2 transmission (forward) transmission (backward) Phase (rad) -2 -3 5000 6000 Frequency (Hz) 5500 6500 7000

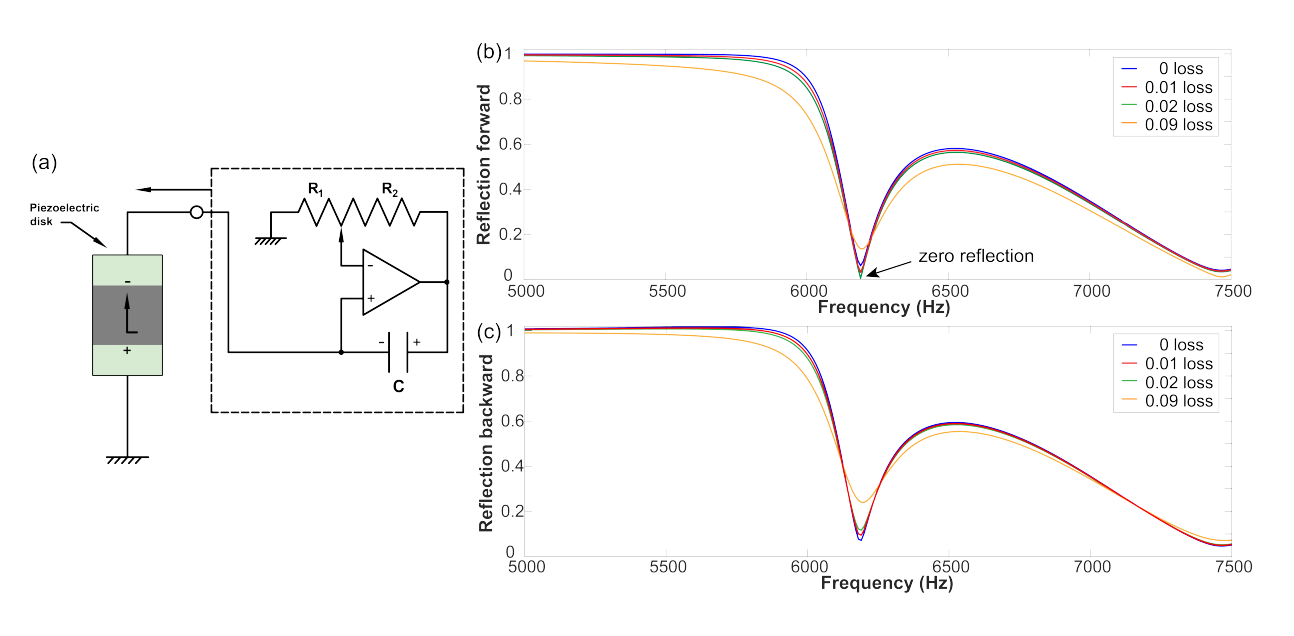
7500

7500



This is the author's peer reviewed, accepted manuscript. However, the online version of record will be different from this version once it has been copyedited and typeset.

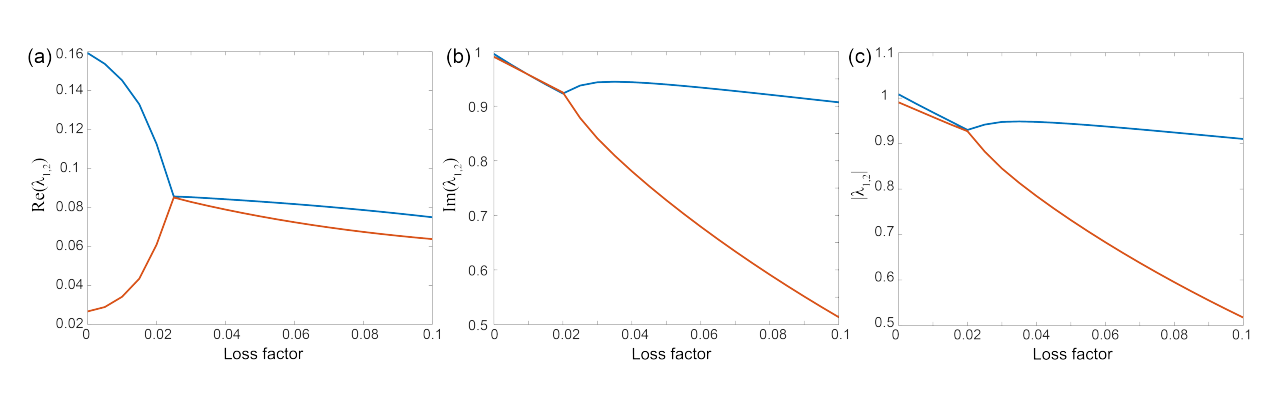
PLEASE CITE THIS ARTICLE AS DOI: 10.1063/5.0097177





This is the author's peer reviewed, accepted manuscript. However, the online version of record will be different from this version once it has been copyedited and typeset.

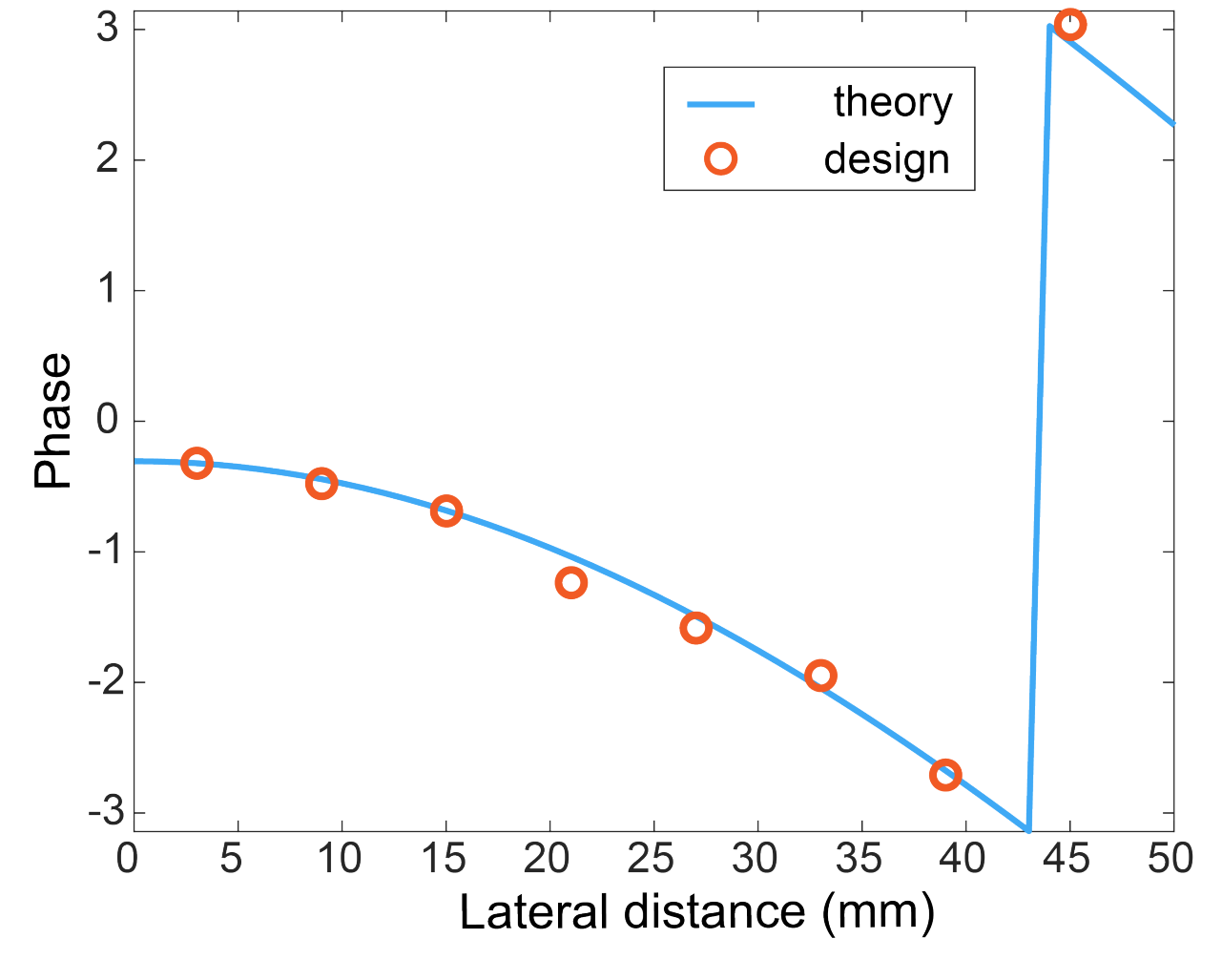
PLEASE CITE THIS ARTICLE AS DOI: 10.1063/5.0097177





This is the author's peer reviewed, accepted manuscript. However, the online version of record will be different from this version once it has been copyedited and typeset.

PLEASE CITE THIS ARTICLE AS DOI: 10.1063/5.0097177





This is the author's peer reviewed, accepted manuscript. However, the online version of record will be different from this version once it has been copyedited and typeset.



